

Structure and Properties of Aluminum Alloy 1421 after Equal-Channel Angular Pressing and Isothermal Rolling

A. A. Mogucheva and R. O. Kaibyshev

Belgorod State University, ul. Pobedy 85, Belgorod, 308015 Russia

Abstract—Sheets from the aluminum alloy 1421 with an ultrafine-grained (UFG) structure and a weak crystallographic texture were prepared by the method of equal-channel angular pressing (ECAP) through a die with channels of a rectangular cross section and by subsequent isothermal rolling. Both operations were carried out at a temperature of 325°C. It is shown that severe plastic deformation (SPD) leads to the formation of a completely recrystallized uniform microstructure with an average grain size of 1.6 μm in the alloy. At room temperature the alloy 1421 demonstrates high static strength ($\sigma_u = 545$ MPa, $\sigma_{0.2} = 370$ MPa) in the absence of a significant anisotropy. At temperatures of hot deformation, the alloy showed ultrahigh elongations under superplasticity (SP) conditions. At a temperature of 450°C and initial deformation rate of $1.4 \times 10^{-2} \text{ s}^{-1}$ the maximum elongation at fracture was ~2700%. At static annealing at a temperature of SP deformation, the UFG structure formed in the process of SPD remains stable. The SP deformation is accompanied by an insignificant grain growth and pore formation.

INTRODUCTION

The weldable Al–Li–Mg alloys are promising for the application in aircraft constructions, since they possess low density, acceptable strength, and high resistance to crack propagation [1, 2]. However, in the coarse-grained state the Al–Li–Mg alloys demonstrate a limited technological plasticity and low service properties, which is connected with the localization of deformation. In addition, there takes place a clearly pronounced anisotropy of mechanical properties, which makes impossible obtaining a whole series of aircraft parts of required quality. The formation of a recrystallized UFG structure in these alloys makes it possible to obtain high strength and plastic characteristics and, which is most important, the isotropy of mechanical properties [1]. Another consequence of the formation of a UFG structure in semifinished products made of Al–Li–Mg alloys is an extraordinary increase in the technological plasticity, which makes it possible to roll these materials into thin sheets and to produce different parts from them using the method of pneumatic forming in the SP state [1, 3, 4]. For these reasons, the development of an industrial technology of production of thin sheets from Al–Li–Mg with a UFG structure is of great practical interest. However, the works performed in the last 30 years clearly showed that this problem does not have satisfactory solution within the framework of the existing technological processes. The traditional thermomechanical treatment (TMT), which consists of cold or hot rolling and recrystallization annealing, is not applicable to Al–Li–Mg

alloys because of their low technological plasticity and crack sensitivity at low temperatures. Consequently, the creation of a technology of producing sheets of Al–Li–Mg of alloys with a completely recrystallized UFG structure is possible only on the base of nontraditional technological processes.

It has been shown in recently published works that the UFG structure in Al–Li–Mg alloys is formed in the process of ECA pressing at elevated temperatures [3–5]. This offers possibility for the creation of the technology of obtaining thin sheets from these alloys which consists of two operations. The first operation is ECA pressing, whose aim is formation of a UFG structure. The second operation is sheet rolling, which provides obtaining parts in the form of sheets. By adjusting optimum values of temperature and the degree and speed of rolling, the rolling can be used for increasing the uniformity of microstructure and, even, for decreasing its anisotropy. However, up to now the technology of ECA pressing made it possible to obtain only samples in the form of bars with a square or round cross section [6, 7], which can be rolled into thin and wide sheets only by using special methods of rolling. It is well known that the classical sheet rolling makes it possible to make thin sheets from plates which have a rectangular cross section; moreover, the width of the plates and sheets must be almost identical. Therefore, in order to create an industrial technology of the production of sheets from Al–Li–Mg alloys with a UFG structure it is necessary to develop such a scheme of ECA pressing which would make it possible to obtain workpieces in the

form of plates. Such workpieces can be prepared using a ECA tool with a rectangular shape of channels [6, 8, 9].

For obtaining isotropic and homogenous structure in high-alloy aluminum alloys, it is necessary that the ECA pressing and the subsequent rolling would be carried out under isothermal conditions at close temperatures [3–5, 9]. This TMT makes it possible to produce thin sheets from aluminum alloys with a UFG structure [12]. It is also worthwhile to note that the rolling, which below is called isothermal rolling, is conducted using rolls heated to the workpiece temperature. In the literature there is no information about the applicability of such two-stage TMT for obtaining thin sheets from Al–Li–Mg alloys. Therefore, the purpose of this investigation was to verify this possibility.

It is shown in this work that thin sheets of the 1421 alloy (Al–Li–Mg–Sc) with a UFG structure can be prepared by the method of ECA pressing with a rectangular shape of channels and subsequent isothermal rolling. In addition, data are given here concerning the influence of TMT on the structure and mechanical properties of sheets of the 1421 alloy at different temperatures. Special attention is given to a study of the characteristics of the superplasticity of these sheets, since they are of great importance for the production of parts of a complex shape by the method of pneumatic forming.

2. EXPERIMENTAL

The aluminum alloy 1421 used in this work has the following chemical composition: Al–5.1% Mg–2.1% Li–0.17% Sc–0.08% Zr; it was obtained by the method of semicontinuous casting and was homogenized at 425°C for 12 h. After this the alloy was subjected to reverse extrusion in the temperature range of 360–390°C with a reduction to 60%.

Workpieces of rectangular shape with dimensions of 125 × 125 × 25 mm were cut out along the axis of the foregoing extrusion and were deformed under isothermal conditions in a tool with an L-like configuration of the channels the angle between which was 90° and the external angle of channel intersection was $\Psi = 0^\circ$ [8, 9]. This configuration provides a true deformation close to 1 per one passage of the workpiece through the channel [8]. The total degree of deformation was defined as the product of the number of passages by the degree of deformation per one pass. The workpiece was undergone to ECA pressing at a temperature of 325°C to a true degree of deformation of ~8; after each passage, the workpiece was turned about the X axis by an angle of 180°; i.e., route C_x [8] was used, in which the picture of shear was equivalent to route C in the traditional ECA pressing [10]. The speed of extrusion was approximately 3 mm/s.

For rolling under isothermal conditions, samples of a rectangular shape cut out from a workpiece subjected

to ECA pressing were used. Their dimensions were 115 × 115 × 15 mm. Before rolling, these workpieces were heated in a furnace to a temperature of 325°C. The rolling was performed under isothermal conditions (with rolls heated to 325°C) to a thickness of 1.8 mm, which made it possible to obtain the total degree of reduction equal to approximately 88% after 8 passages. The isothermal rolling was performed in a six-high cluster mill with the internal rolls 65 mm in diameter and 250 mm in length heated to a temperature of 325°C.

The samples for mechanical tests were cut out in such a way that the direction of tension would coincide with the direction of rolling. The tests were carried out on flat samples with the length of the working part equal to 6 and 10 mm, and with a cross-sectional area of 1.4 × 3 mm². These samples were deformed according to the scheme of equiaxed tension in the range of temperatures of 250–450°C and deformation rates of 10⁻⁴ to 10⁻¹ s⁻¹. At room temperature the samples were deformed at a rate of deformation 5.6 × 10⁻³ s⁻¹. The mechanical tests at room and elevated temperatures were conducted on an Instron-1185 universal dynamometer. For the tensile tests at room temperature, samples were additionally cut out whose working part was inclined at an angle of 45° and 90° to the rolling direction. Prior to the tensile tests at room temperature, the samples were subjected to a standard heat treatment, which consisted of quenching from the temperature of 460°C in oil and subsequent aging at 120°C for 6 h. The other details of mechanical tests were described in [3, 4, 9].

The microstructure and pore formation were studied in the plane parallel to the Z plane (Fig. 1) on the samples deformed by tension to fracture. The region of measurements when studying pore formation in the deformed samples was located at a distance of 5 mm from the fracture surface of the sample. The procedures

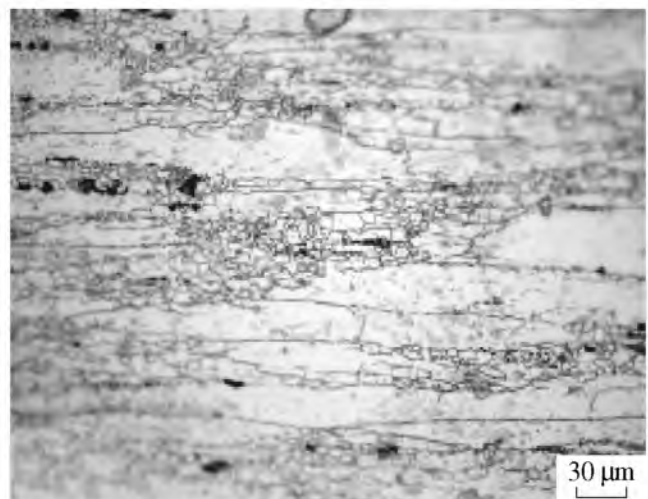


Fig. 1. Initial microstructure of the aluminum alloy 1421.

of optical metallography (OM), transmission electron microscopy (TEM), studying pore formation, and the method of electron back-scatter diffraction (EBSD analysis) are described in detail in the foregoing works [4, 5, 9]. The misorientation of (sub)grain boundaries was determined in a scanning electron microscope (JEOL JSM-840 SEM) equipped with an EBSD attachment (INCA Crystal). The thick and thin lines in the EBSD maps indicate high-angle boundaries (HABs, $\geq 15^\circ$) and low-angle boundaries (LABs, $3^\circ\text{--}15^\circ$), respectively. The electron-microscopic studies of the structure were conducted on a transmission electron microscope (JEOL-2000EX) at an accelerating voltage of 160 kV.

EXPERIMENTAL RESULTS

Microstructure prior to ECA Pressing

The metallographic examination showed that the initial microstructure of the deformed bar of the aluminum alloy 1421 is characterized by a strong inhomogeneity. The structure consists of coarse grains elongated along the direction of extrusion; in their near-boundary regions, pileups of small recrystallized grains are located. The average size of small equiaxed grains is approximately $5\ \mu\text{m}$ (see Fig. 1). The size of the coarse elongated grains is $171\ \mu\text{m}$ in the longitudinal direction and $21\ \mu\text{m}$ in the transverse direction (see Fig. 1).

Microstructure after ECA pressing

After ECA pressing at a temperature of 325°C to a true degree of deformation of ~ 8 there is formed an almost completely recrystallized structure (Fig. 2). Most grain boundaries show clear extinction contours (Fig. 2a), which makes it possible to draw a conclusion about the formation of an equilibrium recrystallized structure. The average dislocation density in the bulk of grains is not great ($\rho = 6 \times 10^{14}\ \text{m}^{-2}$). The volume fraction of recrystallized grains with an average grain size of $1.7\ \mu\text{m}$ is $\sim 85\%$ (Figs. 2b, 2c). Crystallites surrounded by both LABs and HABs are formed (see Fig. 2c). The fraction of recrystallized grains surrounded completely by HABs is $\sim 43\%$ (Fig. 2d). The volume fraction of HABs is equal to $\sim 80\%$, which is characteristic of traditional grain structures [11]. The grain size after ECA pressing through a channel with a rectangular cross section is practically equal to the grain size after traditional ECA pressing [3–5]. The average angle of misorientation at grain boundaries, equal to 33.5° , after the ECA pressing through channels with a rectangular shape of the cross section is nearly the same as after traditional ECA pressing [5]. Note that in [5] the authors considered boundaries with a misorientation of more than 3° as LABs.

Microstructure and the Superplastic Behavior of the 1421 Alloy after ECA Pressing with Subsequent Isothermal Rolling

It is seen from Fig. 3 that the ECA pressing with subsequent isothermal rolling increases the uniformity of the deformed microstructure and the density of lattice dislocations (to $\rho = 6 \times 10^{15}\ \text{m}^{-2}$). The average grain size is equal to $1.6\ \mu\text{m}$. The diffraction patterns (Fig. 3a) represent reflections located on concentric rings, which indicates the presence of predominantly HABs of deformation origin. The fraction of grains completely surrounded by HABs reaches 51% (Fig. 3c). The average angle of misorientation at grain boundaries reaches 35.7° ; the volume fraction of HABs is 85% (Fig. 3d). Note that the fraction of HABs in the aluminum alloy 1421 subjected to isothermal rolling after ECA pressing to a true degree of deformation $e = 8$ is the same as in the alloy deformed by traditional ECA pressing to a true degree of deformation $e = 16$ at the same temperature [5]. At the same time, it should be noted that in the alloy 1421 subjected to ECA pressing through channels with a rectangular cross section and to subsequent isothermal rolling the average grain size is greater than that in the alloy 1421 subjected to classical ECA pressing [3, 4].

The pole figures after ECA extrusion with subsequent isothermal rolling are shown in Fig. 4. It is seen that the ECA pressing with subsequent isothermal rolling leads to a smearing of the texture (Fig. 4).

Typical true-stress–true-strain ($\sigma\text{--}\epsilon$) curves of the alloy 1421 subjected to ECA pressing with subsequent isothermal rolling are displayed in Fig. 5a. The alloy 1421 was deformed by tension at the initial rate of deformation of $1.4 \times 10^{-2}\ \text{s}^{-1}$ in the temperature range of $250\text{--}450^\circ\text{C}$. Figures 5b and 5c depict the $\sigma\text{--}\epsilon$ curves of the alloy deformed at deformation rates from 1.4×10^{-4} to $1.4 \times 10^{-1}\ \text{s}^{-1}$ at temperatures of 300 and 400°C . At $T \geq 300^\circ\text{C}$ and $\dot{\epsilon} \leq 1.4 \times 10^{-2}\ \text{s}^{-1}$ (Fig. 5b), the deformation is accompanied by a steady-state plastic flow, which begins at small degrees of deformation and occurs up to failure, whose nature can be described in the terms of pseudo-brittle fracture. Note that no stage of steady-state flow was observed in either the alloy subjected to traditional ECA pressing [3, 4] or that subjected to ECA pressing with a rectangular channel cross section (Fig. 5d). At low temperatures and high deformation rates after the achievement of maximum the flow stress decreases continuously up to the moment of fracture. The fracture of these samples occurs because of the unsteady plastic flow. An increase in the temperature or a decrease in the rate of deformation leads to a contraction of the stage of the steady-state plastic flow. Note that the flow stresses on the stage of the steady-state deformation of the alloy 1421 subjected to ECA pressing with subsequent isothermal rolling are close to the maximum flow stresses of the alloy 1421 subjected to traditional ECA pressing at $T = 325^\circ\text{C}$ [3, 4].

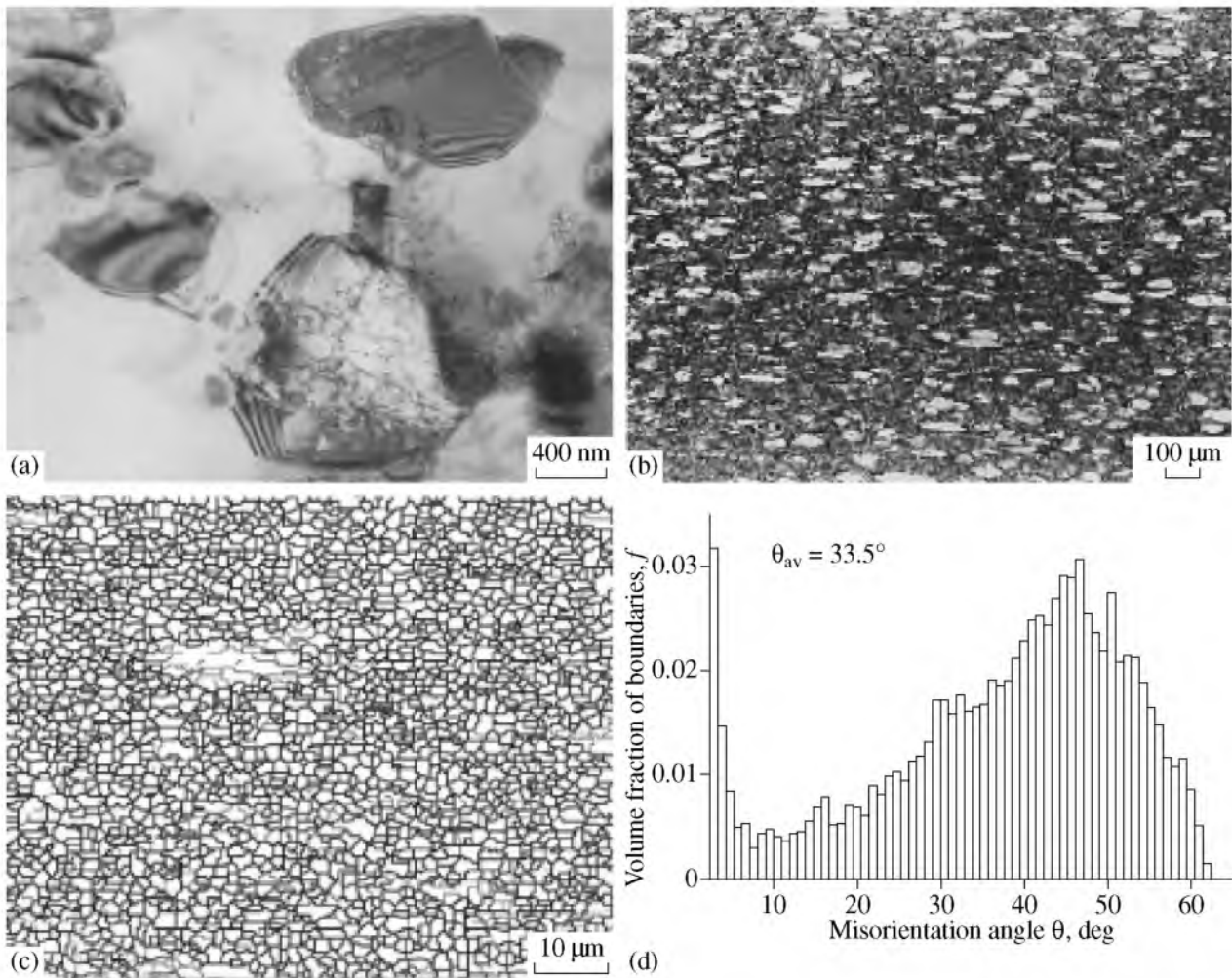


Fig. 2. (a–c) Microstructure of the alloy 1421 after ECA pressing at $T = 325^{\circ}\text{C}$ and $\varepsilon = 8$; and (d) the volume fraction of boundaries versus the angle of misorientation at the boundaries.

In the dependences of the flow stress, relative elongation, and coefficient of strain-rate sensitivity (Fig. 6), there are well distinguished three regions of deformation characteristic of superplastic materials [12, 13]. The σ – ε curves have a sigmoid shape at all temperatures (Fig. 6a). An increase in temperature leads to a displacement of the optimum strain-rate interval of SP [12, 13] to the side of the high deformation rates and to an increase in the values of m from 0.32 at 300°C to 0.57 at 450°C (Figs. 6b, 6c). In the temperature range of 400 – 450°C , the relative elongation of $\geq 1000\%$ is observed in a wide range of strain rates. It is obvious that the alloy 1421 subjected to isothermal rolling after ECA pressing shows high-strain-rate superplasticity. The maximum elongation at fracture (2700%) was observed at a temperature of 450°C and strain rate $\dot{\varepsilon} = 1.4 \times 10^{-2} \text{ s}^{-1}$. The relative elongation of 1000% was observed at the same temperature and at the same deformation rate in the alloy 1421 subjected to ECA pressing. Consequently, the isothermal rolling signifi-

cantly increases the plasticity of the alloy 1421 subjected to ECA pressing with a rectangular shape of the channel cross section. Figure 6d presents the dependence of the true deformation on the coefficient of strain-rate sensitivity at the constant strain rate $\dot{\varepsilon} = 1.4 \times 10^{-2} \text{ s}^{-1}$. In the temperature interval of 400 – 450°C , the values of m increase up to the degree of deformation $\varepsilon \sim 2$. At higher degrees of deformation, upon the passage from the stage of steady-state flow to the stage of softening, there is observed a decrease in m . The high coefficient of strain-rate sensitivity ensures a high resistance of the material to necking and, thus, extraordinary relative elongations.

At $\dot{\varepsilon} = 1.4 \times 10^{-2} \text{ s}^{-1}$, an increase in temperature leads to an increase in both δ and m (Fig. 7). At 250°C , the material shows an average plasticity of 310%, in spite of the low value of $m = 0.2$. Note that there is an uncommon relationship between the coefficient of strain-rate sensitivity and the relative elongation. There is a rigid dependence between m and δ [12] at $m < 0.4$.

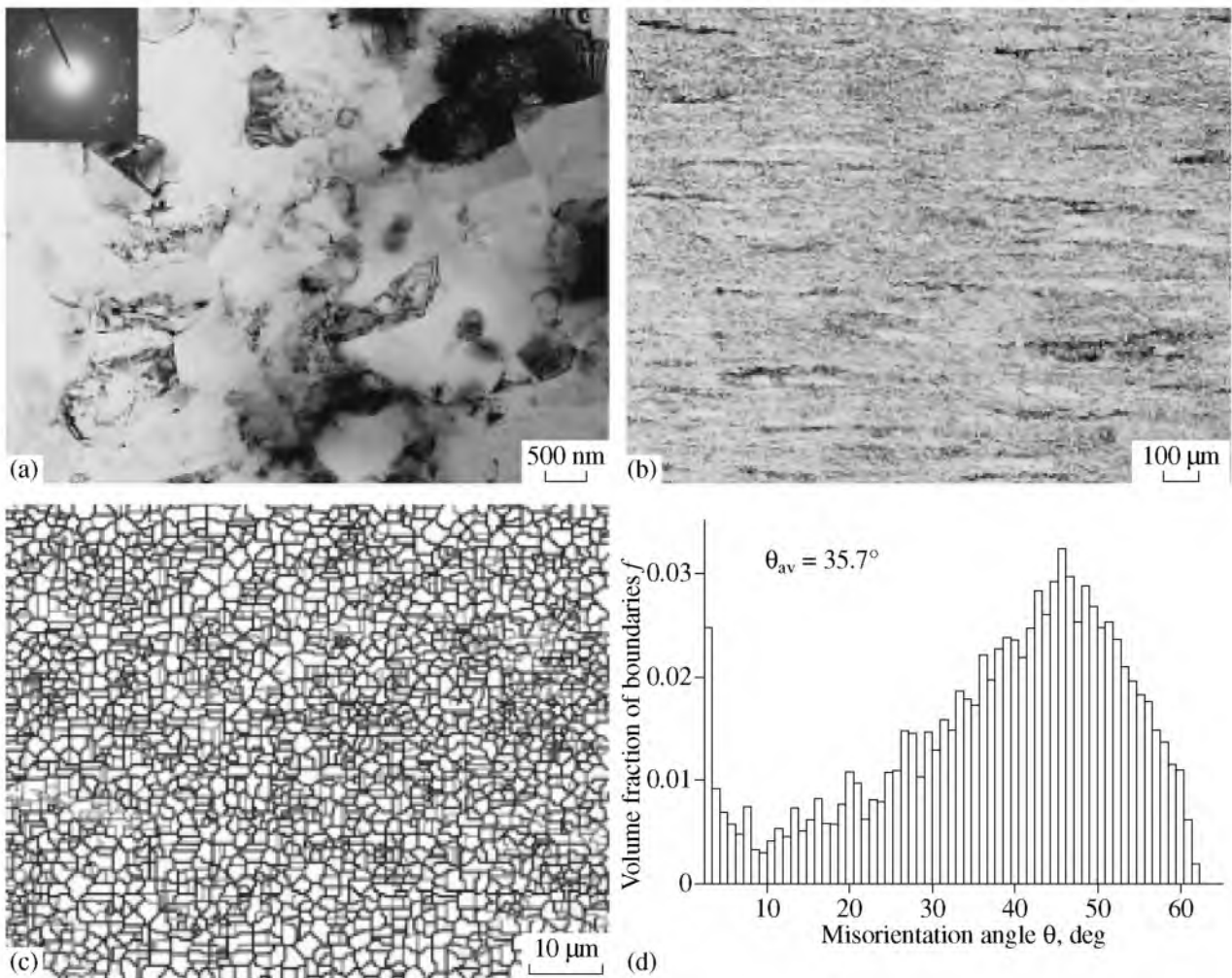


Fig. 3. (a–c) Microstructure of the alloy 1421 after ECA pressing and subsequent isothermal rolling; and (d) distribution of the grain-boundary misorientation angles depending on their volume fraction.

The value of $m = 0.2$ must correspond to a relative elongation which does not exceed 150%. A higher plasticity ($\geq 1000\%$) is observed also at $m \geq 0.4$.

Structural Changes upon Superplastic Deformation

The microstructural changes in the alloy 1421 deformed at a rate of deformation $\dot{\epsilon} = 1.4 \times 10^{-2} \text{ s}^{-1}$ in a temperature range of 350–450°C were studied using regions suffered static annealing (taken from the head of samples) and dynamic annealing (under the conditions for superplastic deformation in the gage parts of the samples). Table 1 displays the average grain size in the gage part (L_D) and in the grip region (L_S), and also the values of the unrecrystallized volume V_{unrecr} . It is seen that the ultrafine grains are sufficiently stable at the static annealing in the temperature interval of 350–450°C. The growth of the recrystallized grains begins only at a temperature of 450°C, which agrees with the data of [4]. In contrast to the aluminum alloy 1421 sub-

jected to classical ECA pressing [4], no growth of unrecrystallized grains is observed in this case. As the temperature of static annealing increases, there is observed a decrease in the fraction of the unrecrystallized structure. Under SP conditions, grain growth is observed. In the temperature range of 350–450°C, the grain sizes in the alloy 1421 after superplastic deformation (see Table 1) and after the superplastic deformation of samples subjected to traditional ECA pressing [4] are similar. Consequently, the isothermal rolling after ECA pressing suppresses growth of the unrecrystallized grains upon static annealing, which increases the stability of fine grains during SP deformation.

In the temperature range of 350–450°C, the fracture occurs as a result of crack propagation at an angle of $\sim 45^\circ$ to the tensile axis. At $T \leq 400^\circ\text{C}$, the pore formation plays an insignificant role in fracture (see Table 1). The volume of pores is $\sim 1\%$; most of them are equiaxed. Consequently, the formation and growth of pores is controlled by diffusion [12]. At a temperature of 450°C, there are formed pores of a serrated shape,

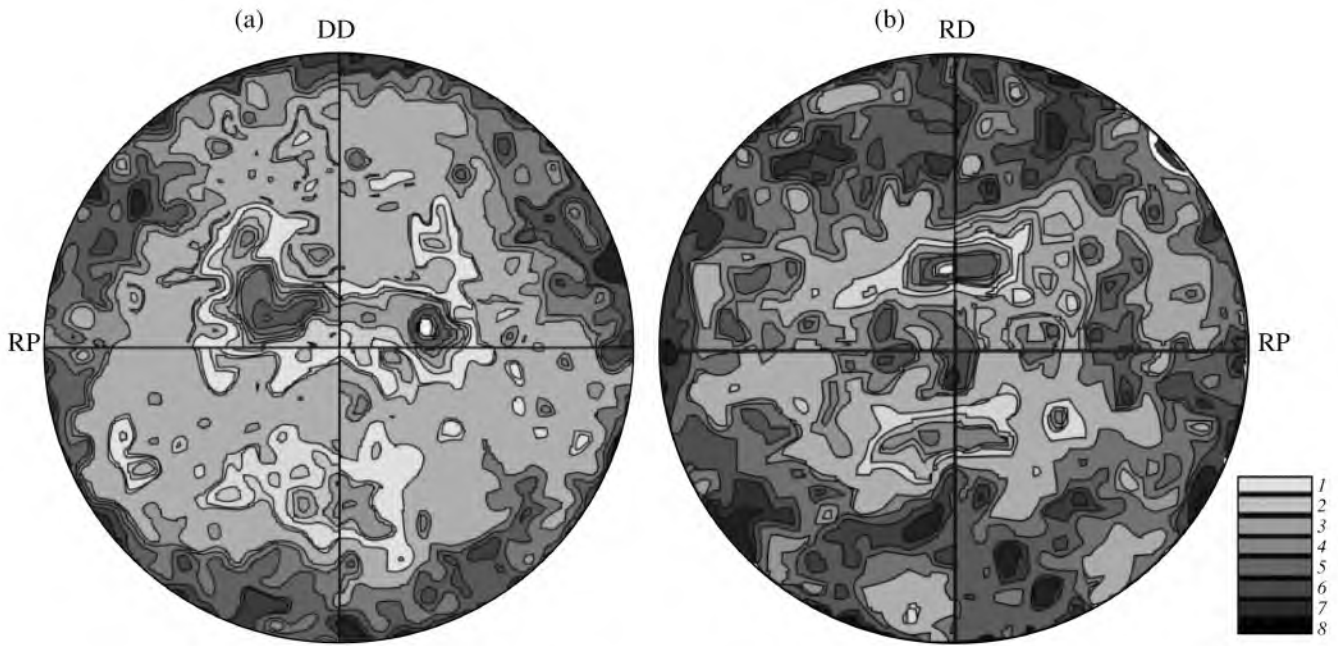


Fig. 4. {111} pole figures of the alloy 1421 after (a) ECA pressing and (b) isothermal rolling.

which indicates the mechanism of their growth controlled by deformation (Fig. 8) [12]. The propagation of a crack between such coarse pores leads to fracture. It is obvious that at a temperature of 450°C the pores play the role of sites for crack formation.

Mechanical Properties at Room Temperature

The typical σ - ϵ curves of alloy 1421 after tensile tests at room temperature are presented in Fig. 9. It is seen that strain hardening ensures uniform plastic deformation up to the moment of fracture. The yield stress, ultimate strength, and plasticity are given in Table 2. The mechanical properties are almost isotropic. For each direction, no less than five samples have been tested, and the difference of the yield stress and ultimate strength was less than 2%, which indicates the high reproducibility of results. The comparison of the data obtained with the data of [14], in which the mechanical properties of the aluminum alloy 1420 with a submicrocrystalline structure were investigated, shows that the alloy 1421 subjected to SPD and subsequent strengthening heat treatment, possesses higher values of the yield stress and ultimate strength. At the same time, the reserve of plasticity of this material is lower than that of the alloy 1421 subjected to classical pressing (17.5%). Such mechanical properties give the possibility for the industrial use of sheets from the alloy 1421 with a UFG structure.

DISCUSSION OF RESULTS

The results of this work show that the use of treatment consisting of ECA pressing and subsequent iso-

thermal rolling makes it possible to produce thin sheets with a UFG structure from the aluminum alloy 1421. After ECA pressing, the alloy acquires high workability and can undergo ultrahigh deformations without the destruction of the workpiece. It is important that in comparison with the traditional ECA pressing ($e \sim 16$) [3, 4], the complex processing used in this work reduces the number of cycles of ECA pressing, since the completely recrystallized structure is formed at a lower total degree of deformation ($e \sim 8$).

In the preceding works [15–17], the sheets of Al-Mg alloys were produced by ECA pressing with subsequent cold rolling. In [16], the traditional ECA pressing was conducted at room temperature; in [15, 17], at 200°C. The last temperature is the temperature of cold deformation for these materials [18]. In [19], it was

Table 1. Average grain size after static annealing (in the region of grips) L_S and after superplastic deformation (in the gage part) L_D ; the volume fraction of the unrecrystallized regions V_{unrecr} ; and the specific volume of pores V_{pore} in the gage part of the samples deformed to fracture at a strain rate of $1.4 \times 10^{-2} \text{ s}^{-1}$ at different temperatures

$T, ^\circ\text{C}$	350	400	450
$L_D, \mu\text{m}^*$	3.5/2.7	4.9/3.6	7.2/5.3
$V_{\text{pore}}, \%$	1.0	1.3	10.1
$L_S, \mu\text{m}$	1.7	2.3	2.8
$V_{\text{unrecr}}, \%$	15	12.4	9.3

* The numerator and denominator represent the grain size measured in the longitudinal and transverse directions, respectively.

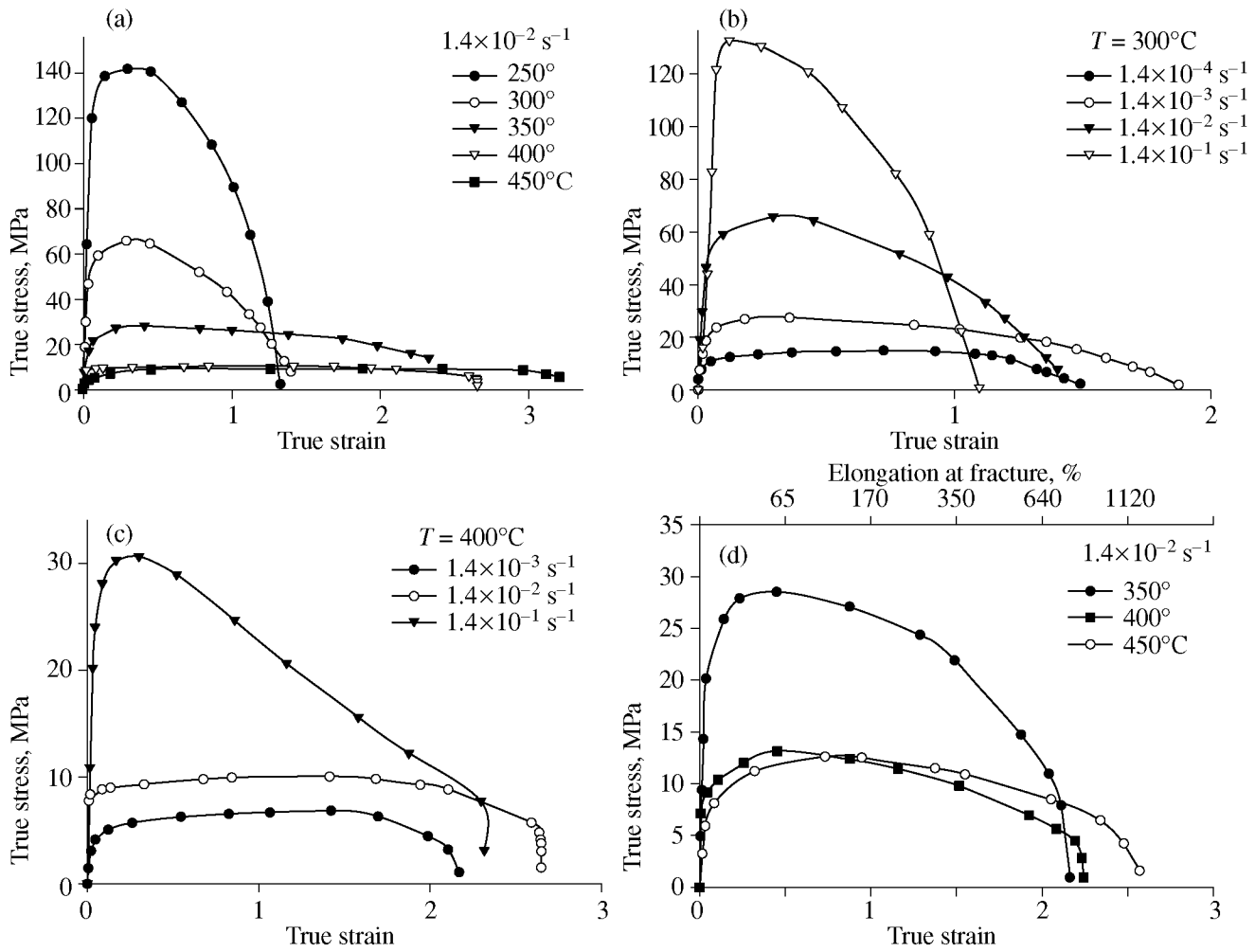


Fig. 5. Dependence of true stresses on true strains for the alloy 1421 obtained at (a) a constant strain rate and (b, c) at a constant temperature of the deformation ((b) $T = 300^\circ\text{C}$; (c) $T = 400^\circ\text{C}$); (d) effect of temperature on the true-stress–true strain curve.

shown that there is no substantial difference in the fraction of HABs that are formed at the equal degree of deformation performed by ECA pressing at room temperature and by cold rolling. The cold rolling following ECA pressing leads to a gradual formation of additional HABs [19]. The formation of a relatively equiaxed fine-grained structure in these materials occurs under the conditions of superplastic deformation as a result of the

development of the process of recrystallization [15, 17].

The enhanced fraction of HABs formed during cold deformation ensures the formation of a more uniform recrystallized structure during subsequent static annealing [20]. As a result, the subsequent rolling of aluminum alloys leads to an improvement of the superplastic properties of alloys processed by ECA pressing [15, 17], or at least the superplastic properties remain actually unchanged [16]. In a given alloy 1421 at a temperature of 325°C the UFG structure with a smeared crystallographic texture (see Fig. 4) is developed directly during SPD. The isothermal rolling after ECA pressing at elevated temperatures accelerates the formation of new HABs. In addition, the smearing of the crystallographic texture in the process of isothermal rolling ensures isotropic mechanical properties at room temperature. Of special importance is the suppression of secondary recrystallization due to growth of elongated unrecrystallized regions. In a homogenous structure with a weak texture and a high fraction of HABs,

Table 2. Effect of the direction of the sample orientation with respect to the axis of tension on the ultimate strength σ_u , yield stress $\sigma_{0.2}$, and relative elongation at fracture δ

Angle to the axis of tension, deg	σ_u , MPa	$\sigma_{0.2}$, MPa	δ , %
0	517	380	14.7
45	538	360	22.2
90	545	370	12.5

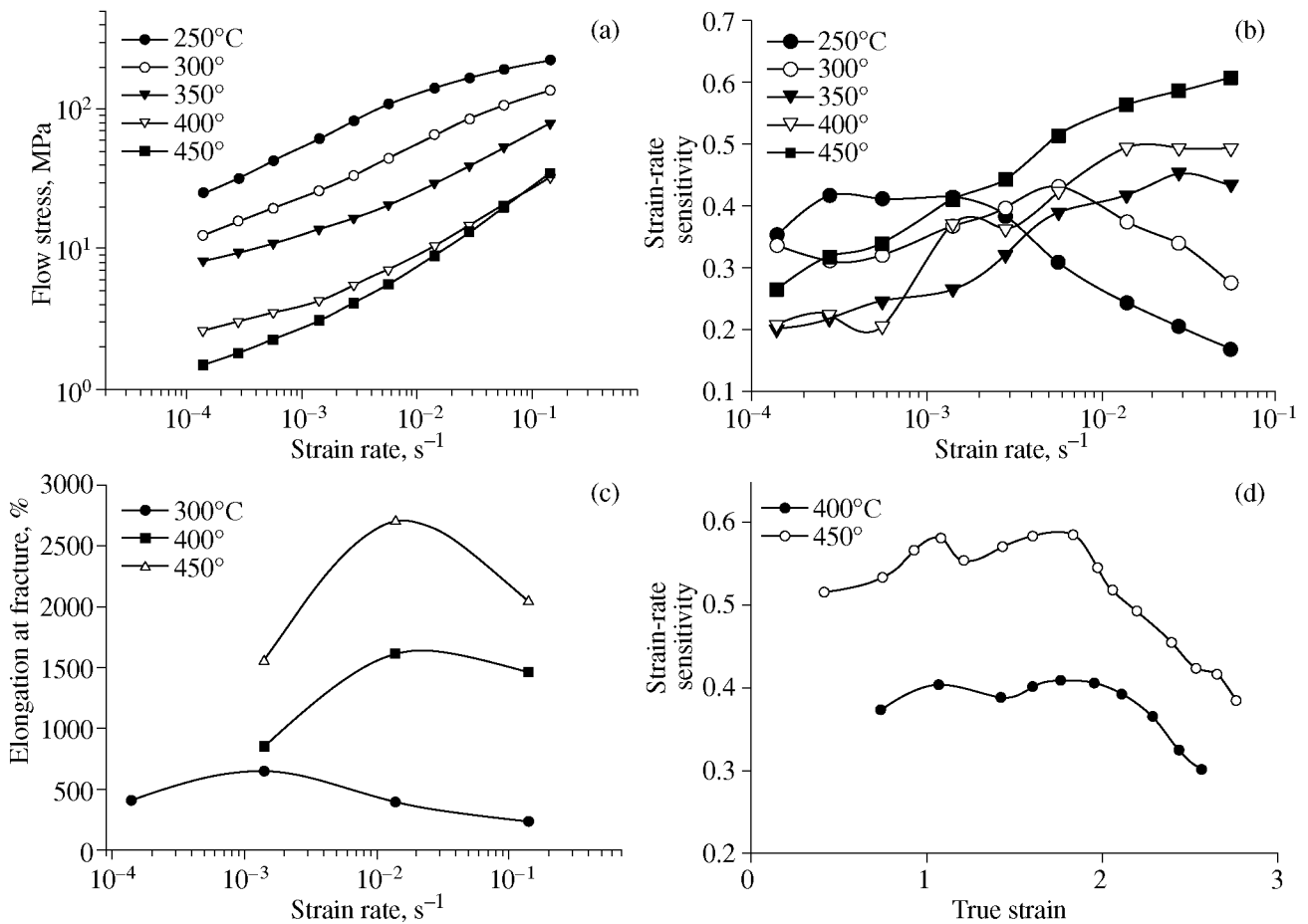


Fig. 6. Effect of the deformation rate on (a) the flow stress, (b) the coefficient of strain-rate sensitivity, and (c) elongation at fracture; and (d) the effect of the degree of deformation on the coefficient of strain-rate sensitivity.

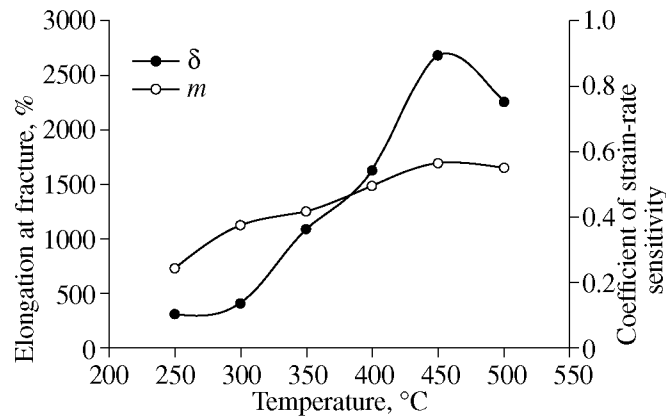


Fig. 7. Elongation at fracture and coefficient of strain-rate sensitivity as functions of the deformation temperature.

only normal static grain growth is possible [21, 22]. As a result, the alloy 1421 with such a structure can be subjected to standard heat treatment including quenching from the temperature of 460°C and subsequent aging without significant grain growth. Consequently, sheets of the alloy 1421 can be used in industry for SP form-

ing, and the parts prepared from them can be subjected to strengthening heat treatments.

The sheets from the alloy 1421 show high mechanical properties at room temperature; their most important feature is the isotropic strength and sufficiently high plasticity. The strength of this alloy 1421 is higher

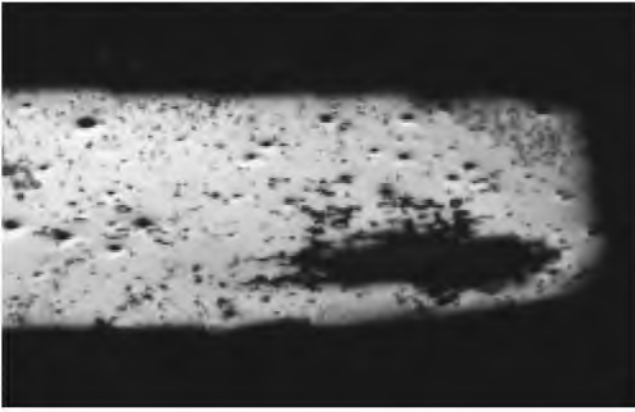


Fig. 8. Pore formation in the sample after ECA pressing with subsequent isothermal rolling during tensile tests at a temperature of 450°C and a strain rate of $1.4 \times 10^{-2} \text{ s}^{-1}$.

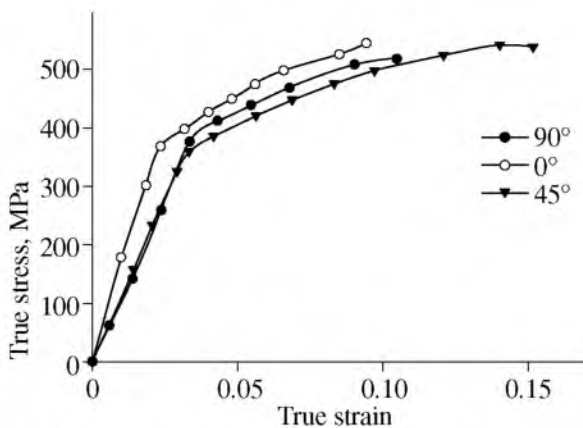


Fig. 9. Dependence of true stress on true strain at room temperature.

than the strength of the alloy AA2524 [23], which is an alloy traditionally employed for commercial airplanes. The plasticity of this alloy 1421 is almost the same as that of the alloy AA2524 [23]. Therefore, taking into account the high resistance to propagation of cracks in the recrystallized state in Al–Li–Mg alloys [1], the sheets from the alloy 1421 with a UFG structure are promising for the applications in the aerospace industry.

Thus, a two-step treatment consisting of ECA pressing and subsequent isothermal rolling is suitable for the industrial production of sheets of the alloy 1421 with high superplastic properties, which are characterized by an excellent combination of strength and plasticity at room temperature. This is connected with the formation of a recrystallized homogenous structure with a weak crystallographic texture as a result of this processing.

CONCLUSIONS

(1) Two-step deformation, which consists of equal-channel angular (ECA) pressing using channels with a

rectangular cross section and subsequent isothermal rolling, ensures the formation of a uniform ultrafine-grained structure in thin sheets of Al–Li–Mg alloys.

(2) An isothermal rolling after ECA pressing increases fraction of high-angle boundaries (HABs) and the fraction of grains surrounded by HABs from all the sides. The fraction of HABs equal to ~85% and the presence of highly dispersed particles of $\text{Al}_3(\text{Sc}, \text{Zr})$ ensure the stability of the UFG structure upon static annealing at temperatures used during severe plastic deformation (SPD).

(3) The alloy 1421 subjected to a two-step deformation shows up high superplastic properties with a maximum elongation at fracture up to ~2700% at a temperature of 450°C, initial strain rate of $1.4 \times 10^{-2} \text{ s}^{-1}$, and appropriate coefficient of strain-rate sensitivity of ~0.57. Such extraordinary properties are connected with the high stability of the arising structure in the process of superplastic deformation.

(4) Depending on the orientation of the samples with respect to the axis of tension, the yield stress, ultimate strength, and elongation at fracture after the standard heat treatment of the alloy 1421 change from 370 to 380 MPa, from 517 to 545 MPa, and from 12.5 to 22%, respectively.

REFERENCES

1. I. N. Fridlyander, K. V. Chuistov, A. L. Berezina, and N. I. Kolobnev, "Aluminum–Lithium Alloys," in *Structure and Properties* (Naukova Dumka, Kiev, 1992) [in Russian].
2. I. N. Fridlyander, L. B. Khokhlatova, N. I. Kolobnev, et al., "Development of Stable Aluminum Alloy 1424 for Applications in Welded Fuselages," *Metalloved. Term. Obrab. Met.*, No. 1, 1–9 (2002).
3. F. Musin, R. Kaibyshev, Y. Motohashi, et al., "High Strain Rate Superplasticity in an Al–Li–Mg Alloy Subjected to Equal-Channel Angular Extrusion," *Mater. Trans.* **43** (10), 2370–2377 (2002).
4. R. Kaibyshev, K. Shipilova, F. Musin, and Y. Motohashi, "Achieving High Strain Rate Superplasticity in an Al–Li–Mg–Sc Alloy through Equal-Channel Angular Extrusion," *Mater. Sci. Technol.* **21** (4), 408–418 (2005).
5. R. Kaibyshev, K. Shipilova, F. Musin, and Y. Motohashi, "Continuous Dynamic Recrystallization in an Al–Li–Mg–Sc Alloy during Equal-Channel Angular Extrusion," *Mater. Sci. Eng., A* **396**, 341–351 (2005).
6. V. M. Segal, "Engineering and Commercialization of Equal Channel Angular Extrusion," *Mater. Sci. Eng., A* **386**, 269–276 (2004).
7. R. Z. Valiev, R. K. Islamgaliev, and I. V. Alexandrov, "Bulk Nanostructured Materials from Severe Plastic Deformation," *Prog. Mater. Sci.* **45**, 103–189 (2000).
8. M. Kamachi, M. Furukawa, Z. Horita, and T. G. Langdon, "Equal-Channel Angular Pressing Using Plate Samples," *Mater. Sci. Eng., A* **361**, 258–266 (2003).
9. I. Nikulin, R. Kaibyshev, and T. Sakai, "Superplasticity in a 7055 Aluminum Alloy Processed by ECAE and Sub-

- sequent Isothermal Rolling,” *Mater. Sci. Eng., A* **407**, 62–70 (2005).
10. Z. Horita, M. Furukawa, M. Nemoto, and T. G. Langdon, “Development of Fine Grained Structures Using Severe Plastic Deformation,” *Mater. Sci. Technol.* **16**, 1239–1245 (2000).
 11. F. J. Humphreys, P. B. Prangnell, J. R. Bowen, et al., “Developing Stable Fine-Grain Microstructures by Large Strain Deformation,” *Philos. Trans. R. Soc. London A* **357**, 1663–1681 (1999).
 12. J. Pilling and N. Ridley, *Superplasticity in Crystalline Solids* (The Institute of Metals, London, 1989).
 13. O. A. Kaibyshev, *Superplasticity of Alloys, Intermetallics, and Ceramics* (Springer, Berlin, 1992).
 14. M. Furukawa, Z. Horita, M. Nemoto, et al., “Factors Influencing the Flow and Hardness of Materials with Ultrafine Grain Sizes,” *Philos. Mag.* **78** (1), 203–215 (1998).
 15. K. T. Park, H. J. Lee, C. S. Lee, et al., “Enhancement of High Strain Rate Superplastic Elongation of a Modified 5154 Al by Subsequent Rolling after Equal Channel Angular Pressing,” *Scr. Mater.* **51**, 479–483 (2004).
 16. H. Akamatsu, T. Fujinami, Z. Horita, and T. G. Langdon, “Influence of Rolling on the Superplastic Behavior of an Al–Mg–Sc Alloy after ECAP,” *Scr. Mater.* **44**, 759–764 (2001).
 17. K. T. Park, H. J. Lee, Ch. S. Lee, and D. H. Shin, “Effect of Post-Rolling after ECAP on Deformation Behavior of ECAPed Commercial Al–Mg Alloy at 723 K,” *Mater. Sci. Eng., A* **393**, 118–124 (2005).
 18. R. Kaibyshev, F. Musin, E. Avtokratova, and Y. Motohashi, “Deformation Behavior of a Modified 5083 Aluminum Alloy,” *Mater. Sci. Eng., A* **392**, 373–379 (2005).
 19. O. V. Mishin, D. Juul Jensen, and N. Hansen, “Microstructures and Boundary Populations in Materials Produced by Equal Channel Angular Extrusion,” *Mater. Sci. Eng., A* **342**, 320–328 (2003).
 20. H. Jazaeri and F. J. Humphreys, “The Transition from Discontinuous to Continuous Recrystallization in Some Aluminium Alloys: I. The Deformed State,” *Acta Mater.* **52**, 3239–3250 (2004).
 21. H. Jazaeri and F. J. Humphreys, “The Transition from Discontinuous to Continuous Recrystallization in Some Aluminium Alloys: II. Annealing Behaviour,” *Acta Mater.* **52**, 3251–3262 (2004).
 22. M. Ferry, N. E. Hamilton, and F. J. Humphreys, “Continuous and Discontinuous Grain Coarsening in a Fine-Grained Particle-Containing Al–Sc Alloy,” *Acta Mater.* **53**, 1079–1109 (2005).
 23. V. I. Elagin, “The State and the Ways of Enhancement of Fracture Strength of High-Strength Aluminum Alloys,” *Metalloved. Term. Obrab. Met.*, No. 9, 10–17 (2002).

SPELL: 1. angleof, 2. sigmoid